Phase space volume conservation under space and time discretization schemes for the shallow-water equations

MATTHIAS SOMMER *

Freie Universität Berlin, Institut für Meteorologie, Carl-Heinrich-Becker-Weg 6–10, D-12165 Berlin, Germany

SEBASTIAN REICH

Universität Potsdam, Institut für Mathematik, Am Neuen Palais 10, D-14469 Potsdam, Germany

ABSTRACT

It has recently been proposed to apply concepts of analytical mechanics to numerical discretization techniques for geophysical flows. So far, mostly the role of the conservation laws for energy and vorticity based quantities has been discussed but recently the conservation of phase space volume has also been addressed. This topic relates directly to questions in statistical fluid mechanics and in ensemble weather and climate forecasting. Here, we investigate phase space volume behaviour of different spatial and temporal discretization schemes for the shallow-water equations on the sphere. We compare combinations of spatially symmetric and common temporal discretizations. Furthermore, the relation between time-reversibility and long-time volume averages is addressed.

1. Introduction

In atmospheric modeling, many properties of a numerical scheme contribute to its overall performance. Local accuracy of the operators, numerical stability, phase speed of characteristic waves and conservation laws for mass, momentum, energy and vorticity based quantities have long been a matter of interest (see, for example, Arakawa (1966); Vichnevetsky and Bowles (1982); Salmon (1983); Zeitlin (1991); Salmon (2005); Sommer and Névir (2009)). In related efforts, new classes of numerical schemes have been developed for classical mechanics (Leimkuhler and Reich (2004), Hairer et al. (2006). Of particular interest in this field are conservation laws for energy, symmetry induced conservation laws, and preservation of the symplectic structure. These methods, primarily designed for finite dimensional systems of ordinary differential equations, are now commonly referred to as geometric integration. Extension of geometric integration to Hamiltonian partial differential equations (Morrison (1998); Shepherd (1990); Salmon (1999)) is still an active area of research (Bridges and Reich (2006)). See Frank and Reich (2004) for a particular application to atmospheric fluid dynamics.

In this paper, we focus on a particular aspect of geometric integration methods; namely conservation of volume and time-reversibility (Arnold (1989)). Considering inviscid atmospheric dynamics as a dissipation-free dynamical system, phase space volume is expected to be conserved. This is a reasonable assumption even though this system is not symplectic but Lie-Poisson (Arnold (1989)). It should be emphasised that the relation of volume conservation to reversibility is delicate (Lamb 1996; Posch and Hoover 2004). In particular, time-reversibility does not imply volume conservation but as will be shown below sets close boundaries to fluctuations.

There are practical applications where phase space volume behavior of a given dynamical system can be of relevance. When computing ensemble forecasts, a spurious phase space contraction or expansion respectively could have severe effects on the implied ensemble spread and the dimension of the chaotic attractor (Ehrendorfer (1994a,b)). Possibly, this lack of conservation is most dominant for the most unstable dimensions, i. e. those with the largest Lyapunov exponents.

The aim of this article is to investigate the impact of common spatial and temporal discretization schemes of a 'state of the art' atmospheric forecast model on phase space volume and its relation to time-reversible discretization methods (Leimkuhler and Reich (2004), Hairer et al. (2006)). This topic has been previously addressed in Egger (1996). Dubinkina and Frank (2007) showed that the Arakawa scheme (Arakawa (1966)) for two-dimensional incompressible flow is volume conserving. Here we show results of a more general physical and numerical setting.

Section 2 gives a definition of phase space volume conservation for numerical schemes in terms of the Liouville equation and introduce the concept of time-reversibility. In section 3, three different spatial discretization schemes

of the shallow-water equations on the sphere are compared regarding their phase space volume conservation properties. In section 4, different time-integration schemes are compared.

2. Volume conservation under numerical discretizations

For this analysis, the discretization process is understood as split into two parts, namely *spatial* (e. g. finite differences) and *temporal* (e. g. implicit midpoint, leap-frog) discretization. This carries a partial differential equation (PDE) over to an ordinary differential equation (ODE) and to an algebraic equation (AE).

a. Volume conservation and time-reversibility under spatial discretization

For a given PDE

$$\dot{z} = \mathbf{X}_{\text{PDE}}[z] \tag{1}$$

let the ODE

$$\dot{z} = \mathbf{X}(z) \tag{2}$$

be a spatially discretized approximation of that PDE (1). The corresponding normalised probability density function $\rho(z(t), t)$ is defined to fulfil the Liouville equation

$$\partial_t \rho = -\nabla \cdot (\rho \mathbf{X}) \quad \text{or equivalently} \quad \frac{\mathrm{d}\rho}{\mathrm{d}t} = -\rho \,\mathrm{div}\,(\mathbf{X}). \tag{3}$$

This evolution equation can be interpreted as a conservation law for the probability p of finding a system in a given co-moving volume $V(t)$:

$$\frac{\mathrm{d}}{\mathrm{d}t} \underbrace{\int_{V(t)} \mathrm{d}V \, \rho}_{=:p} = 0. \tag{4}$$

Locally, $\mathrm{d}p = \rho \mathrm{d}V$ and thus the phase space volume is antiproportional to the density ρ. In the following when speaking about phase space volume, what is meant is simply the inverse of the density.

Generally, the divergence of the discretized equation (2) need not be the same as that of the field equation (1). We define the difference as the accuracy order of volume conservation of that specific spatial discretization:

$$\mathrm{div}\,(\mathbf{X}_{\text{PDE}}) = \mathrm{div}\,(\mathbf{X}) + \mathcal{O}(\Delta x^r). \tag{5}$$

A PDE (1) is called time-reversible, if there is a linear transformation of variables S such that $S = S^{-1}$ and $\mathbf{X}_{\text{PDE}}(Sz) = -S\mathbf{X}_{\text{PDE}}(z)$. Similarly, a finite-dimensional spatial truncation (2) is called time-reversible if $\mathbf{X}(Sz) = -S\mathbf{X}(z)$. Time-reversibility of a PDE is relatively easy to

maintain under spatial discretizations except for the advection terms (Egger (1996)). In this paper, we consider only spatial discretizations which lead to reversible ODEs (2). See Section 3.

As a Hamiltonian system, the shallow-water equations and the incompressible Euler equations have vanishing divergence. Generally it is considered to be impossible to spatially truncate the Hamiltonian PDEs of fluid mechanics to a finite dimensional Hamiltonian system. While the antisymmetry condition can be maintained by discretizing the Poisson brackets, this method does not ensure the Jacobi identity to be fulfilled. A notable exception is provided by Zeitlin's truncation of the 2D incompressible Euler equations (Zeitlin (1991)). On the other hand, one may abandon the Hamiltonian nature of (1) and seek volume only conserving discretrizations instead. Indeed, Arakawa's discretization for the 2D incompressible Euler equations is time-reversible and also conserves volume (Dubinkina and Frank (2007)). However, it should be noted that time-reversibility does not imply conservation of volume, in general (Lamb (1996)), and we will demonstrate this fact numerically in Section 3.

b. Volume conservation under temporal discretization

In the following, the accuracy order of volume conservation for time stepping algorithms of linear systems is considered. Experiments with the nonlinear shallow-water equations in Section 4 will partially reflect this linear analysis but also feature important differences. For now, assume the ODE (2) to be linear:

$$\dot{z} = Az \tag{6}$$

with constant phase space divergence

$$\mathrm{div}\,(Az) = \mathrm{tr}(A).$$

Let M be the specific discrete flow map that maps the prognostic variables $z_i = z(t_i)$ from timestep i to $i + 1$:

$$M : z_i \mapsto Mz_i = z_{i+1}. \tag{7}$$

According to assumption (4) the probability p is constant in a co-moving control volume so that

$$\int_{V_{i+1}} \mathrm{d}V_{i+1} \, \rho(z_{i+1}, t_{i+1}) = \int_{V_i} \mathrm{d}V_i \, \rho(z_i, t_i)$$

and the left hand side complies with the transformation formula

$$\int_{V_{i+1}} \mathrm{d}V_{i+1} \, \rho(z_{i+1}, t_{i+1}) = \int_{V_i} \mathrm{d}V_i \, \rho(Mz_i, t_{i+1}) \det(M)$$

so that

$$\rho_{i+1} \det(M) = \rho_i. \tag{8}$$

Here, the abbreviation $\rho_i := \rho(z_i, t_i)$ has been used. Since M is the discrete flow map of an s order time integration scheme, it satisfies

$$M = \exp(\Delta t A + \mathcal{O}(\Delta t^{s+1})).$$

Also, eq. (8) can be written as a discrete Liouville equation

$$\frac{\rho_{i+1} - \rho_i}{\Delta t} = -\frac{\rho_i}{\Delta t}(1 - \frac{1}{\det M}) \tag{9}$$

$$= -\frac{\rho_i}{\Delta t}(1 - \exp(-\mathrm{tr}(\Delta t A + \mathcal{O}(\Delta t^{s+1})))). \tag{10}$$

A comparison of this to the exact solution

$$\frac{\hat{\rho}_{i+1} - \rho_i}{\Delta t} = -\frac{\rho_i}{\Delta t}(1 - \exp(-\mathrm{tr} A \Delta t)) \tag{11}$$

shows that the accuracy order of volume conservation is also s. While s designates the order of accuracy of volume tendency, the volume ratio between two time steps is actually of order $s + 1$.

1) TIME-REVERSIBLE SYSTEMS

We now demonstrate that conservation of volume for linear systems (6) is closely linked to the conservation of time-reversibility under a numerical time-stepping method (7).

In a typical situation of fluid dynamics, where the nonlinear equations of motion are invariant under time reflection, the corresponding linear system (6) satisfies

$$SA = -AS, \tag{12}$$

where S acts by inverting the sign of the velocity components. Then the eigenvalues of A come in pairs with opposite signs since

$$SA\mathbf{v} = \lambda S\mathbf{v} = -AS\mathbf{v}.$$

Hence, assuming that A is diagonalisable, A is a traceless matrix. Therefore in the linear case, time-reversibility and volume conservation are equivalent. If a discrete flow map

$$z_{i+1} = Mz_i$$

satisfies the corresponding symmetry

$$SM = M^{-1}S, \tag{13}$$

then $\det M = 1$ and volume is conserved. Condition (13) is satisfied for symmetric Runge-Kutta methods such as the implicit midpoint/trapezoidal rule. It does not hold for non-symmetric methods such as explicit and implicit Euler and the popular explicit fourth-order Runge-Kutta methods (Leimkuhler and Reich (2004) and Hairer et al. (2006)).

The situation becomes more complicated for general nonlinear ODEs (2) with time-reversing symmetries. It can be shown (Reich (1999)) that symmetric Runge-Kutta methods can be interpreted as the "exact" solution to a modified ODE

$$\dot{z} = \widehat{\mathbf{X}}_{\Delta t}(z)$$

which satisfied $S\widehat{\mathbf{X}}_{\Delta t}(z) = -\widehat{\mathbf{X}}_{\Delta t}(Sz)$, i.e., the modified ODE is still time-reversible. However, since time-reversibility does *not* imply conservation of volume for nonlinear ODEs, the same applies to numerical methods. We will explore this issue further in the subsequent section and Section 4.

c. Volume conservation in terms of Lyapunov exponents

Recall that the Lyapunov exponents $\lambda_1, \ldots, \lambda_N$ of an N-dimensional dynamical system (2) are defined as

$$\lambda_j = \lim_{t \to \infty} \frac{1}{t} \ln \sigma_j(x, t),$$

where $\sigma_1, \ldots, \sigma_N$ are the singular values of the Jacobi matrix of the flow map.

The sum of the Lyapunov exponents satisfies

$$\sum_j \lambda_j = \lim_{t \to \infty} \frac{1}{t} \int_0^t \mathrm{div}\, \mathbf{X}(z(t')) \mathrm{d}t', \tag{14}$$

which, for ergodic systems, is equal to the phase space or ensemble mean.

For a time-discretized system $z_{i+1} = \phi(z_i)$, this reads

$$\sum_j \lambda_j = \lim_{k \to \infty} \frac{1}{k} \sum_{i=0}^{k-1} \ln |\det J_z(\phi(z_i))|$$

$$= \lim_{k \to \infty} \frac{1}{k} \ln \prod_{i=0}^{k-1} |\det J_z(\phi(z_i))|,$$

where $J_z(\phi(z))$ denotes the Jacobian of ϕ at z, and therefore

$$e^{\sum_j \lambda_j} = \lim_{k \to \infty} \prod_{i=0}^{k-1} |\det J_z(\phi(z_i))|^{\frac{1}{k}} = \lim_{k \to \infty} \sqrt[k]{\frac{\rho_0}{\rho_k}}$$

$$= \lim_{k \to \infty} \overline{\{\frac{\rho_i}{\rho_{i+1}}\}_{0 \le i \le k}}, \tag{15}$$

where the overbar denotes the geometric mean. It is assumed that no re-orientation takes place, which is reasonably the case here.

For conservative systems, phase space volume is conserved and therefore the sum of all Lyapunov exponents equal to zero. For systems with volume expansion or contraction, this sum is shifted to a positive respectively a negative value. For time-reversible systems, the sum of the

Lyapunov exponents is zero generically. [1] Consequently (14) states that as long as reversibility is ensured, phase space volume is conserved in a long-term average even if locally the vector fields are not divergence free. The same applies to time-reversible maps. In other words, a symmetric time integration scheme with a reversible space discretization can be expected to average out local fluctuations in volume over long time simulations.

3. Experiments with spatial discretization schemes

In this section, three different spatial discretization schemes of the shallow-water equations on a staggered inhomogeneous triangular grid (the ICON grid) will be compared. One is the ICON shallow-water prototype (ICOSWP), a finite volume scheme with wind and height as prognostic quantities. The second (Helmholtz) is also a finite volume scheme but with prognostic quantities vorticity, divergence and height. The third (Nambu) predicts also vorticity, divergence and height and has additionally algebraic exact conservation properties for total energy and potential enstrophy. A detailed description of these schemes can be found in Sommer and Névir (2009).

For the Nambu scheme (see Sommer and Névir (2009) for notation), the divergence of the prediction vector field in phase space can be explicitly computed as

$$\text{div}\,(\mathbf{X}_{\text{Nambu}}) = \frac{2}{9} \sum_l \frac{\lambda_l}{\delta_l} \partial_l^\perp \gamma \frac{1}{\partial_l^\perp \overline{q}} (\widetilde{q}(\widetilde{\frac{1}{A_\nu \overline{h}_\nu}})_l - q(\widetilde{\frac{1}{A_\nu \overline{h}_\nu}})_l) \neq 0.$$
(16)

As a difference of the product of a mean and the mean of a product, this spatial semi-discretization is not exactly divergence-free and even a perfectly volume preserving time integration method would not preserve phase space volume. The divergent part of the prognostic vector field is due to compressibility and the grid inhomogeneity. Neglecting this, phase space divergence vanishes for the same reason as stated in Dubinkina and Frank (2007). However, the divergence (16) vanishes in the continuous limit and is very small for practical choices of resolution as shown below.

To keep the results independent of the number of grid points N, instead of displaying volume ratio, the (geometric) mean length expansion respectively contraction ratio

$$\Lambda_{i,j} := \sqrt[N]{\frac{\rho_j}{\rho_i}}$$

will be used. This can be interpreted as a typical length of the observed volume in one dimension, or as the geometric

---

[1] A non-zero sum of Lyapunov exponents for time-reversible systems is possible for systems with a strong local violation of volume conservation and leads to the existence of low dimensional attractors and repellors (Posch and Hoover 2004).

mean ensemble variation. The relation to the Lyapunov exponents is

$$e^{\frac{1}{N} \sum_j \lambda_j} = \lim_{k \to \infty} \overline{\{\Lambda_{i,i+1}\}_{0 \le i \le k}}$$
(17)

according to (15). It must be stressed though, that even with conserved total volume, the variation may be very different in the distinct dimensions as the volume deforms. To determine variation along the different dimensions, an ensemble forecast would be the appropriate method.
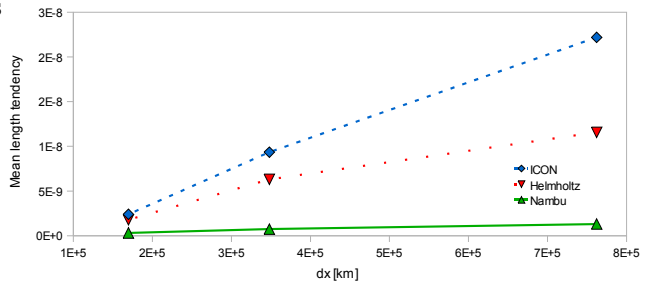

FIG. 1. Mean length tendency against grid constant. ICON (dashed), Helmholtz (dotted) and Nambu (solid) scheme.

Mean length tendency as given by $\frac{1}{N}\text{div}\,(\mathbf{X})$ against spatial resolution is depicted in figure 1 for three different spatial discretization schemes on the ICON grid. Due to the complexity of the problem, only three values (corresponding to 802, 3202 and 12802 data points respectively) were computed. With more data available, the order of spatial accuracy r could be determined. For the comparison between the different spatial and temporal schemes we focus on the absolute values however. Obviously all three schemes are not divergence-free, in contrast to the results for the tendency of potential enstrophy. For that quantity it has been shown in Sommer and Névir (2009), that the tendency of the Nambu scheme vanishes algebraically. Still, all schemes considered here converge and, as will be shown below, volume non-conservation is still rather small compared to that caused by asymmetric time integration schemes.

4. Experiments with temporal discretization schemes

In this section, different time-integration rules are compared concerning their volume conservation properties. The spatial scheme chosen here is the ICON scheme, but any other choice gives very similar results. The spatial resolution for these tests was set at 800km, corresponding to the lowest resolution in the previous section.

a. Implicit mid-point rule

The implicit mid-point rule

$$z_{i+1} = \phi(z_i) = z_i + \Delta t \mathbf{X}\left(\frac{z_{i+1} + z_i}{2}\right)$$

is symmetric and therefore conserves volume very well, whenever the underlying ODE is reversible (Egger (1996)). Here we show experimentally, that while the conservation property is well reproduced, it is not exact. Vanishing phase space divergence is not a sufficient criterion for volume conservation under this scheme (Hairer et al. 2006). As discussed in Section 1, volume is conserved exactly for linear time-reversible systems , since the implicit midpoint is time-reversible. Note also that volume conservation for general Hamiltonian systems can be ensured by using symplectic time integration methods (Leimkuhler and Reich 2004; Hairer et al. 2006). An application of such a method for the shallow-water equations on the sphere is given in Frank and Reich (2004).
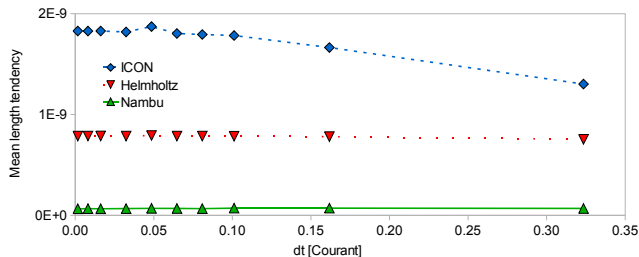

FIG. 2. Mean length tendency for the implicit midpoint scheme. ICON (dashed), Helmholtz (dotted) and Nambu (solid) scheme.

Mean length tendency according to (9) against time step size is plotted in Fig. 2 for different spatial discretization schemes. It can be seen that the non-conservation of volume is dominated by the spatial truncation error.

b. Leap-frog method

As shown in Egger (1996) the unfiltered leap-frog scheme is symmetric and volume conserving in the extended phase space, even for non-reversible equations. Here we show results of the leap-frog with Asselin filter, a common method to control the computational mode. This filter makes the scheme asymmetric and the volume contraction rate can be computed as:

$$\frac{\rho_{i+1}}{\rho_i} = (1 - 2\gamma)^{-N},$$

where γ is the Asselin parameter and N the number of grid points. This yields a discrete Liouville equation of the form

$$\frac{\rho_{i+1} - \rho_i}{\Delta t} = -\frac{\rho_i}{\Delta t}\left(-2N\gamma + \mathcal{O}(\gamma^2)\right).$$

This is independent of the generating vector field and time-step size, therefore no reasonable accuracy order can be given for this scheme. However, for typical choices of time-step and Asselin parameter values (0.02 has been chosen here), phase space volume is distinctively contracted within only a few time steps, see Fig. 3.
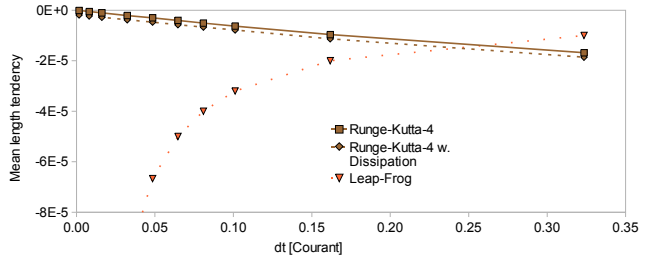

FIG. 3. Mean length tendency for Leap-frog (dotted) and Runge-Kutta-4 time integration (inviscid: solid, viscid: dashed).

c. Fourth-order Runge-Kutta scheme

While for the linearised equations, volume conservation under this scheme is of fourth-order accuracy, the results of an experiment (Fig. 3) with the nonlinear equations suggests a very different behavior. Comparing this to the results of the experiments with the symmetric implicit midpoint scheme, the fourth order explicit Runge-Kutta scheme shows strong volume contraction even for reasonably small time step sizes. To give an impression of the scale of this phenomenon, the result of the same experiment with added viscosity of the form $\nu\nabla^2\mathbf{v}$ ($\nu = 10\frac{\text{km}^2}{\text{s}}$, corresponding to an e-folding time of the smallest wave numbers representable on the grid of half a day) is also displayed in Fig. 3. As expected, the dissipation leads to a volume contraction; here about 3 per cent in 3 hours. 1 per mil of energy is dissipated over the same period. While volume contraction due to this viscosity is much stronger than the effect of spatial discretization on volume, it is small compared to the effect of the temporal discretization scheme. This shows clearly, that volume non-conservation by numerical schemes can be comparable or even larger than the effect of the physical processes involved.

5. Conclusion

Focusing on the divergence-free example of the shallow-water equations, phase space volume behavior for different discretization schemes has been analysed. For the spatial discretization, it was found that none of the three schemes tested is a divergence-free approximation, which is due to the variable staggering and the inhomogeneity of the grid.

Concerning the time integration methods, it was found that only the symmetric implicit midpoint scheme comes

close to volume conservation. In combination with a reversible (but not necessarily divergence-free) space discretization this symmetric scheme ensures time-averaged volume conservation. All other schemes showed significant spurious volume contraction, dominating the effects of space discretization and even that of viscosity. While phase space volume (non-)conservation is an abstract property of any dynamical system, the degree of its numerical realization can obviously have an important impact on results of the ensemble forecasting method. The above mentioned shortcomings will eventually cause a systematic error in ensemble spread.

The implicit midpoint/trapezoidal rule shows a desirable behavior with regard to conservation of volume; but it is very expensive to implement. While computationally efficient standard implementations of semi-implicit variants (Durran (1998)) are no longer symmetric, a framework for time-symmetric semi-implicit methods have recently been proposed (Staniforth et al. (2007); Reich (2006); Hundertmark and Reich (2007)). These methods should display the same desirable behavior with regard to time-averaged volume conservation as the implicit midpoint/trapezoidal rule.

REFERENCES

Arakawa, A., 1966: Computational design for long-term numerical integration of the equations of fluid motion: Two-dimensional incompressible flow. Part I. *J. Comput. Phys.*, **1**, 119–143.

Arnold, V., 1989: *Mathematical Methods of Classical Mechanics.* 2d ed., Springer-Verlag, New York.

Bridges, T. J. and S. Reich, 2006: Numerical methods for Hamiltonian PDEs. *Journal of Physics A: Mathematical and General*, **39 (19)**, 5287–5320.

Dubinkina, S. and J. Frank, 2007: Statistical mechanics of Arakawa's discretizations. *J. Comput. Phys.*, **227 (2)**, 1286–1305.

Durran, D., 1998: *Numerical Methods for Wave Equations in Geophysical Fluid Dynamics.* Springer-Verlag, Berlin Heidelberg.

Egger, J., 1996: Volume conservation in phase space: A fresh look at numerical integration schemes. *Mon. Wea. Rev.*, **124**, 1955–1964.

Ehrendorfer, M., 1994a: The Liouville-equation and its potential usefulness for the prediction of forecast skill. part I: Theory. *Mon. Wea. Rev.*, **122**, 703 – 713.

Ehrendorfer, M., 1994b: The Liouville-equation and its potential usefulness for the prediction of forecast skill. part II: Applications. *Mon. Wea. Rev.*, **122**, 714 – 728.

Frank, J. and S. Reich, 2004: The Hamiltonian particle-mesh method for the spherical shallow water equations. *Atmospheric Science Letters*, **5**, 89–95.

Hairer, E., C. Lubich, and G. Wanner, 2006: *Geometric numerical integration.* 2d ed., Springer, 515 pp.

Hundertmark, T. and S. Reich, 2007: A regularization approach for a vertical-slice model and semi-Lagrangian Störmer-Verlet time stepping. *Q.J. Royal Met. Soc.*, **133 (627)**, 1575–1587.

Lamb, J. S. W., 1996: Area-preserving dynamics that is not reversible. *Physica A: Statistical and Theoretical Physics*, **228 (1-4)**, 344 – 365.

Leimkuhler, B. and S. Reich, 2004: *Simulating Hamiltonian Dynamics.* Cambridge University Press, 379 pp.

Morrison, P., 1998: Hamiltonian description of the ideal fluid. *Rev. Modern Phys.*, **70**, 467–521.

Posch, H. and W. Hoover, 2004: Large-system phase space dimensionality loss in stationary heat flows. *Physica D*, **187**, 281–293.

Reich, S., 1999: Backward error analysis for numerical integrators. *SIAM J. Numer. Anal.*, **36**, 475–491.

Reich, S., 2006: Linearly implicit time stepping methods for numerical weather prediction. *BIT*, **46**, 607–616.

Salmon, R., 1983: Practical use of Hamilton's principle. *J. Fluid Mech.*, **132**, 431–444.

Salmon, R., 1999: *Lectures on Geophysical Fluid Dynamics.* Oxford University Press, Oxford.

Salmon, R., 2005: A general method for conserving quantities related to potential vorticity in numerical models. *Nonlinearity*, **18**, R1–R16.

Shepherd, T., 1990: Symmetries, conservation laws, and Hamiltonian structure in geophysical fluid dynamics. *Adv. Geophys.*, **32**, 287–338.

Sommer, M. and P. Névir, 2009: A conservative scheme for the shallow-water system on a staggered geodesic grid based on a Nambu representation. *Quart. J. Roy. Meteor. Soc.*, **135**, 485–494.

Staniforth, A., N. Wood, and S. Reich, 2007: A time-staggered semi-Lagrangian discretization of the rotating shallow-water equations. *Quart. J. Roy. Meteor. Soc.*, **132**, 3107–3116.

Vichnevetsky, R. and J. Bowles, 1982: *Fourier analysis of numerical approximations of hyperbolic equations.* SIAM, Philadelphia.

Zeitlin, V., 1991: Finite-mode analogs of 2D ideal hydrodynamcis: Coadjoint orbits and local canonical structure. *Physica D*, **49**, 353–362.